ELSEVIER

Polymer Vol. 37 No. 9, pp. 1669–1675, 1996

0032-3861/96/$15.00 + 0.00

Direct comparison of the segmental orientations of free oligomer and network chains in polybutadiene model networks

Marly M. Jacobi
Instituto de Quimica, Universidade Federal de Rio Grande do Sul, Avenida Bento Goncalves 9500, 91501-970 Porto Alegre, Brazil

and Volker Abetz* and Reimund Stadler
Institut für Organische Chemie, Johannes Gutenberg-Universität, J. J. Becher Weg 18–20, 55099 Mainz, Germany

and Wolfram Gronski
Institut für Makromolekulare Chemie, Albert-Ludwigs-Universität, Stefan Meier Strasse 31, 79104 Freiburg, Germany
(Received 6 September 1995; revised 19 November 1995)

The segmental orientation in a semi-interpenetrating polymer network based on crosslinked polybutadiene swollen to different degrees by free butadiene oligomers (of molar masses below the entanglement limit) is studied as a function of uniaxial strain for both the oligomer chains and the network chains by using ^{2}H nuclear magnetic resonance (n.m.r.) spectroscopy. While the second moment of the orientation distribution function, P_2, is usually obtained from the quadrupolar splitting of the maxima of the spectra, herein we obtain the averaged P_2 from the whole spectrum. For high volume fractions of the network chains ($\phi > 0.8$) the untangled oligomer shows the same degree of orientation as the network, while for larger degrees of swelling the oligomer orientation is smaller than that of the network chains. Strain birefringence measurements performed on the same materials show a similar strain dependence as the orientation parameter obtained from ^{2}H n.m.r. spectroscopy. Copyright © 1996 Elsevier Science Ltd.

(Keywords: segmental orientation, ^{2}H n.m.r. spectroscopy; polybutadiene networks)

INTRODUCTION

There has been much interest and controversy regarding the importance of segmental correlations on the orientational behaviour of flexible polymers in both the melt and in networks. Some intriguing experiments were performed by Deloche and Samulski[1]. They observed a quadrupolar splitting $\Delta\nu$ in the ^{2}H n.m.r. spectra of a deuterated solute probe which was swollen into a deformed elastomer network. The origin of this $\Delta\nu$ derives from the orientation of the network. Subsequent ^{2}H n.m.r. spectroscopic investigations carried out by Deloche, Samulski and coworkers[2–8] on deuterated polydimethylsiloxane (PDMS) networks swollen with free nondeuterated PDMS chains and on free deuterated PDMS chains swollen into non-deuterated PDMS networks indicated that, for low volume fractions of the free chains (large ϕ, with ϕ being the volume fraction of the network chains), the $\Delta\nu$ (D_n) associated with the network and that of the solvent chains were of the same magnitude. Thus, assuming the quadrupolar splittings are a measure of orientation, it was concluded that both the network and the oligomeric swelling agent have the same degree of orientation. The degree of orientational correlation between the probe and the matrix can be quantified by an orientational coupling parameter ϵ. This parameter relates the orientation of the (mechanically) completely relaxed swelling probe f_p and the orientation of the mechanically non-relaxed matrix (network) f_n as follows:

$$f_p = \epsilon f_n \tag{1}$$

According to these ^{2}H n.m.r. spectroscopic results ϵ would be close to unity. Such a high value of the orientational coupling must be compared to the considerably lower values obtained for other systems using other methods. A value of $\epsilon \sim 0.4$ was obtained from infra-red (i.r.)-dichroism and birefringence experiments on mixtures of entangled high- and low-molecular-weight polymers[9,10] and selectively labelled homopolymers[11]. A more recent study on blends and semi-interpenetrating networks of non-deuterated high-molecular-weight polybutadiene or polybutadiene networks with deuterated oligobutadienes of various degrees of polymerization, showed that the orientational coupling parameter is a function of the degree of polymerization of the oligomer. Systems with strongly entangled oligomers

* To whom correspondence should be addressed

($M_{probe} > 10\,M_e$) show a value of ϵ of *c.* 0.4, while a decrease of the oligomer molecular weight leads to an increase of ϵ up to a value of unity for small oligomers below the entanglement limit ($M_{probe} < M_2$)[12]. Since a rather detailed survey of the literature on orientational coupling between solvents and polymers, oligomers and polymers and different labelled blocks within a polymer is given in ref. 12, we will not go into any further details here.

Concerning the interpretation of the ^{2}H n.m.r. spectra, there is an ongoing discussion about the origin of the observed line shapes in deformed labelled elastomers[6,13–17]. These line shapes cannot be represented by the superposition of just two Lorentzian functions. A superposition of only two Lorentzian functions would occur if: (i) only one type of C–D bond with very fast dynamics with respect to the n.m.r. time-scale ($\sim 10^{-7}$ s) is present in the system and (ii) all C–D bonds show the same average degree of orientation. Poon and Samulski recently analysed some of the original PDMS data[2] in terms of a distribution of motional rates for segmental reorientation by using a single orientation parameter[14] and alternatively, with the assumption that a distribution of quadrupolar interactions is averaged by a single reorientational process[15]. While both attempts successfully describe the endlinked PDMS networks with only small deformations, this cannot explain the origin of the strong broadening observed in the deformed polybutadiene networks. In one of our former papers on deuterated polybutadiene networks[13] it was assumed that complete motional averaging occurs. The spectra could then be simulated for a non-averaged distribution of segmental orientations of the C–D bonds, which were attributed to different orientations of network chains of various lengths. Such an analysis implies an inhomogeneous distribution of mechanical stress among the different network chains. However, a complete analysis of the lineshapes in the deformed polybutadienes must account for the fact that the CD_2 methylene units neighbouring *cis* ($-CD_2-C_c=$) and *trans* ($-CD_2-C_t=$) double bonds show differently averaged bond orientations with respect to the end-to-end vector[18–20]. Different theoretical attempts to simultaneously explain the line broadening and the quadrupolar splitting of the ^{2}H n.m.r. spectra have been developed independently by Deloche and Sotta[16] and Brereton[17]. According to these approaches the splitting can only be observed in the presence of nematic coupling[16] or an anisotropic excluded volume potential[17]. Another explanation for the unusual line shapes in PDMS networks[7,8] could be based on dynamical differences between network chains, dangling chain ends and free probe chains[21]. According to Kornfield *et al.*[21], the observed splitting is due to the signal of the mobile dangling chain ends, which experience the same degree of coupling as the free probes. This should explain the apparent discrepency between the values of ϵ observed by ^{2}H n.m.r. spectroscopy[7,8,18] and i.r.-dichroism[9,10]. However, this explanation is in contradiction to the experimental results in ref. 13, where similar ^{2}H n.m.r. spectra were obtained although, as a result of the very high molecular weight of the primary chains after crosslinking, the amount of dangling chain ends is negligible.

Herein we will show another method of data analysis of ^{2}H n.m.r. spectra for the determination of orientation and compare these results with those obtained by taking into account only the quadrupolar splitting between the maxima. The n.m.r. spectroscopic data will be compared with data obtained from birefringence, which can be regarded as an independent method. In addition, it will be shown that this analysis gives a high orientational coupling parameter ($\epsilon \sim 1$) for semi-interpenetrating networks of polybutadiene swollen to various degrees with oligobutadienes which have molecular masses below the entanglement mass.

EXPERIMENTAL

^{2}H n.m.r. spectroscopic experiments were performed using a Bruker CXP 300 spectrometer operating at a frequency of 46.073 MHz. The spectra of the deformed networks were taken with the magnetic field parallel to the stretching direction. All spectra were acquired at room temperature using the solid echo pulse sequence[22]. The 90° pulse had a length of 6 μs. The number of scans (1000–3000) was adjusted to obtain an adequate signal-to-noise ratio.

Birefringence measurements were performed on an Instron 1122 tensile testing machine equipped with a He–Ne laser operating at 632.8 nm and two crossed polarizers oriented at 45° and −45° with respect to the strain axis[23].

Details of the anionic synthesis of the high-molecular-weight deuterated polybutadiene and the deuterated polybutadiene oligomers, as well as details of the network synthesis, are given elsewhere[24–27]. *Table 1* summarizes the characteristics of the linear polybutadiene used for network synthesis, as well as details for the oligomers. *Table 2* gives the results obtained from characterization of the network. The crosslink density was determined from the stress–strain behaviour, analysed either by the Mooney–Rivlin equation or the Flory–Erman theory[24,28–30].

Samples of 35–40 mm length and 5 mm width (thickness *c.* 0.3 mm) were cut from the bulk crosslinked network sheets. The appropriate amount of oligomer was distributed on top of the sample and allowed to penetrate into the network. Homogeneous swelling of the network by the oligomer was achieved after about 3 days. The exact volume fractions were determined gravimetrically by assuming volume additivity. The samples were stored in the refrigerator to avoid additional

Table 1 Characteristics of high- and low-molecular-weight polybutadienes

Sample	M_n (g mol^{-1})	M_w/M_n [a] (g mol^{-1})	Degree of deuteration[b] (%)
Deuterated precursor of network	370 000[c]	1.41	65–70
Deuterated oligomer	990[d], 800[e]	1.17	65–70
Protonated oligomer	750[d], 730[e]	1.114	0

[a] Obtained by size exclusion chromatography
[b] Degree of deuteration, with respect to C(1) and C(4) of butadiene ($C(D,H)_2=CH-CH=C(D,H)_2$), determined by ^{1}H n.m.r. Microstructure: 7% 1,2-units, 93% 1,4-units, approximately equally distributed as *cis* and *trans*[23–25]
[c] Obtained by membrane osmometry
[d] Obtained by vapour pressure osmometry
[e] Obtained by ^{1}H n.m.r. end-group analysis

Table 2 Characteristics of the polybutadiene network

Mooney–Rivlin analysis		Flory–Erman junction constraint theory		
$2C_1$ ($N\,mm^{-2}$)	M_c ($g\,mol^{-1}$)	Number density of elastically effective junctions ($mol\,l^{-1}$)	M_c ($g\,mol^{-1}$)	Chain ends (%)
0.253	4400	1.33×10^{-4}	3380	0.9–1.2

thermal crosslinking. They were fixed at the end in a manually driven strain device mounted in an n.m.r. tube, and the deformation ratio was obtained by measuring the distance between markers on the sample. In order to ensure mechanical equilibrium, several spectra were recorded after different times. No changes in the spectra were obtained with time for these networks.

The network orientation was obtained directly from measurements on the deuterated network which has been swollen by non-deuterated oligomer, while the oligomer orientation was obtained by extraction from the difference between the spectra obtained from the network swollen by deuterated and by non-deuterated oligomer. Calculation of these difference spectra was carried out in the time domain (free induction decay, $FID(t)$) before Fourier transformation into the frequency domain after normalizing the two measurements with respect to each other, as follows:

$$FID_{\phi,\lambda}^{N_dO_n}(t)_{norm} = \frac{FID_{\phi,\lambda}^{N_dO_n}(0)}{FID_{\phi,\lambda}^{N_dO_d}(0)} FID_{\phi,\lambda}^{N_dO_d}(t) \qquad (2)$$

where N_d is the deuterated network, O_d and O_n are the deuterated and non-deuterated oligomers, respectively, λ is the strain ratio, and ϕ is the volume fraction of the network chains.Therefore, the FID of the pure oligomer was obtained according to the following:

$$FID_{\phi,\lambda}^{O_d}(t) = FID_{\phi,\lambda}^{N_dO_d}(t)_{norm} - \phi FID_{\phi,\lambda}^{N_dO_n} \qquad (3)$$

The main advantage of this procedure as compared to the calculation of the difference spectra in the frequency domain are: (i) that the overall intensity ($FID(0)$) is obtained independently from setting any integration limits, (ii) errors due to baseline imperfections are negligible, and (iii) an enhanced speed of data processing.

RESULTS AND DISCUSSION

Figure 1 shows typical sets of ^2H n.m.r. for: the deuterated polybutadiene network swollen by deuterated oligomer (a), the deuterated network swollen by non-deuterated oligomer (b) and the resulting difference spectra for the deuterated oligomer (c), for a network volume fraction of $\phi = 0.8$. The spectra obtained for the oligomer from the subtraction method are similar to those obtained directly from deuterated oligomer in a non-deuterated network[18]. Deformation of the network leads to a quadrupolar splitting of two pairs of doublets. The inner splitting is assigned to the C–D bonds of the methylene units neighbouring *cis*-configurational double bonds, while the outer splitting corresponds to the methylene units neighbouring *trans*-configurational double bonds. This is known from T_1 relaxation time measurements[25] and Monte Carlo simulations based on the rotational isomeric state model[19,20,31]. A knowledge of the microstructure is essential if the orientation

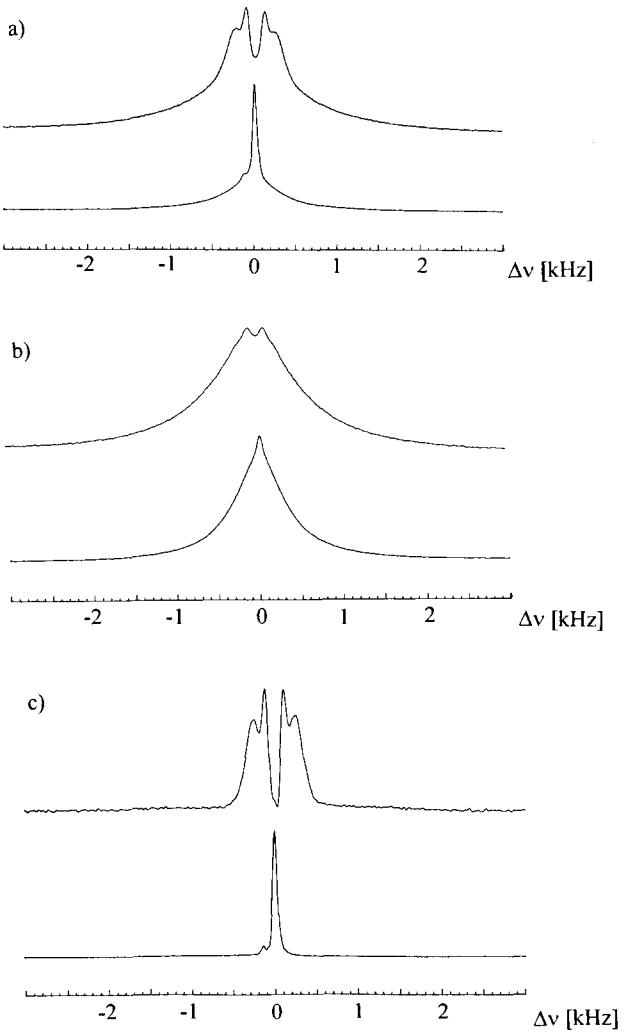

Figure 1 ^2H n.m.r. spectra for a network with 20% oligomer ($\phi = 0.8$) at different strain ratios (upper curve at $\lambda = 1.5$, lower curves at $\lambda = 1$): (a) network with deuterated oligomer; (b) network with protonated oligomer; (c) difference spectra for the deuterated oligomer

parameter for statistical segments $<P_2(\cos\theta)>$, is to be determined, since the relative orientation of the C–D bonds to the statistical segment $<P_2(\cos\gamma)>$ relates $<P_2(\cos\theta)>$ to the measurable $<P_2(\cos\alpha)>$ via the addition theorem for Legendre polynomials, as follows:

$$<P_2(\cos\alpha)> = <P_2(\cos\theta)><P_2(\cos\gamma)> \qquad (4)$$

where α is the angle between the C–D bond and the stretching direction (in the case of ^2H n.m.r. spectroscopy), or the long axis of the refractive index tensor (in the case of birefringence), and the stretching direction, θ is the angle between the statistical segment (local chain axis) and the stretching direction, and γ is the angle between the C–D bond (in the case of ^2H n.m.r. spectroscopy), or the long axis of the refractive index

tensor (in the case of birefringence), and the local chain axis. Since the determination of $<P_2(\cos\gamma)>$ requires knowledge about the local chain structure, we focus on $<P_2(\cos\alpha)>$, since this quantity can be directly obtained experimentally. For a particular microstructure, $P_2(\cos\alpha)$ can be obtained from the quadrupolar splitting of a doublet $\Delta\nu_{max}$ according to the following:

$$P_2(\cos\alpha) = \frac{\Delta\nu_{max}}{2\delta P_2(\cos\Omega)} \tag{5}$$

where Ω is the angle between the stretching direction and the magnetic field and δ is the quadrupolar coupling constant (125 kHz for aliphatic C–D bonds[32]). Note that equation (5) does not yield an ensemble average value for $P_2(\cos\alpha)$ because $\Delta\nu_{max}$ corresponds to the most probable orientation of the units for a particular microstructure. Since the spectral intensity is distributed over a broad range of frequencies, the whole spectrum, rather than only $\Delta\nu_{max}$, is considered in order to obtain an ensembled averaged moment $<P_2(\cos\alpha)>$. This is achieved by calculating the averaged moment $<(\cos\alpha)^2>$ using the following ($\Omega = 0°$):

$$<(\cos\alpha)^2> = \frac{1}{3}\frac{\sum_{|\Delta\nu|=0}^{\delta} I(\Delta\nu)\left(\frac{\Delta\nu}{\delta}+1\right)^{\frac{1}{2}}}{\sum_{|\Delta\nu|=0}^{\delta} I(\Delta\nu)\left(\frac{\Delta\nu}{\delta}+1\right)^{-\frac{1}{2}}} \tag{6}$$

which is obtained by variable substitution from the following equation:

$$<(\cos\alpha)^2> = \frac{\sum_{0}^{\pi/2} I(\alpha)(\cos\alpha)^2\sin\alpha}{\sum_{0}^{\pi/2} I(\alpha)\sin\alpha} \tag{7}$$

and equation (5). In equation (6) $I(\Delta\nu)$ is a time averaged value, since the reorientational dynamics in the system are faster than the n.m.r. time scale. From equation (6) the second-order Legendre polynomial can be calculated, by using tabulated values for the coefficients[33], as follows:

$$<P_2(\cos\alpha)> = \frac{1}{2}(3 < \cos^2\alpha > -1) \tag{8}$$

By this treatment differentiation between the different microstructures units is omitted, but average values for the orientation parameters are obtained for all of the C–D bonds. Since the chemical microstructure is the same for both the network and the oligomers, this omission should not affect the determination of the orientational coupling parameter. An additional advantage of this approach is that the orientation parameter can be determined in spectra at low deformations where no visible quadrupolar splitting of the maxima can be resolved in the spectra. To evaluate the correct orientation parameter the sign of $\Delta\nu$ must also be known. This can be determined by varying the angle Ω between the stretching direction and the magnetic field from 0 to 90°. For the systems under study here the observed $\Delta\nu$ values are in fact negative, because the quadrupolar splitting is larger for $\Omega = 90°$ than for $\Omega = 0°$ ($\Delta\nu_{90°} = 2\Delta\nu_{0°}$). This is due to the orientation of the C–D bonds which are at an angle larger than the magic angle (54.7°) with respect to the main chain axis; it is the main chain axis which aligns parallel to the stretching direction for a perfectly oriented system. In *Figure 2* values of $<P_2(\cos\alpha)>$ *versus* the strain function (with λ = length/initial length) are shown for both the network and oligomer. It can be seen that $<P_2(\cos\alpha)>$ for the oligomer is almost zero for the isotropic unstrained sample. This is the same value which is expected for C–D bonds which are oriented at the magic angle. On the other hand, an 'orientation' of the network, which is caused by a spectral line broadening due to incomplete motional averaging, is observed in the unstretched state. Assuming an independence of the motional and orientational effects one would expect a broad line to appear also when the stretching direction and the magnetic field enclose the magic angle (MA). Under this condition all orientational effects vanish in the spectrum and only line broadening due to incomplete motional averaging remains. The mathematical treatment for separating the dynamical contributions from the orientational contributions to the spectra would be a deconvolution, which can be carried out by a division of the spectra in the time domain (free induction decay) as follows:

$$FID^{corr}_{\Omega,\lambda}(t) = \frac{FID_{\Omega,\lambda}(t)}{FID_{MA,\lambda}(t)} \tag{9}$$

The Fourier transform of $FID^{corr}_{\Omega,\lambda}(t)$ yields the spectrum where all motions are averaged completely. However for our experiments[26], it was not possible to perform measurements at the magic angle. More recently, similar experiments have been performed on thermoplastic elastomers and it was found that the line shape changes only very little with strain[34] for measurements at the magic angle. Therefore, we will discuss only the variation of the different Legendre polynomials with respect to the unstrained state, i.e.

$$\Delta < P_2(\cos\alpha)_\lambda > = <P_2(\cos\alpha)_\lambda>_{exp} - <P_2(\cos\alpha)_1>_{exp} \tag{10}$$

This is possible since the experimentally determined $<P_2(\cos\alpha)_1>_{exp}$ contains the contribution due to incomplete motional averaging. *Figure 3* shows the values of the order parameter according to equation

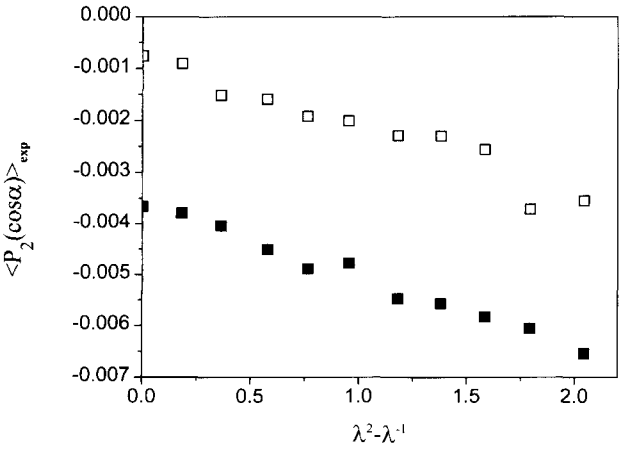

Figure 2 $<P_2(\cos\alpha)>_{exp}$ *versus* the strain function for both network (■) and oligomer (□) when $\phi = 0.8$

(10) for two samples with different degrees of swelling. While oligomer and network chains show the same values in the case where $\phi = 0.8$, a smaller orientation for the oligomer is found for $\phi = 0.6$. This indicates a concentration dependence of the orientational coupling parameter, which is determined from the slope of plots such as those shown in *Figure 4*, where oligomer orientation is shown as a function of network orientation.

Birefringence measurements on these samples were used as an independent method to determine orientation. Birefringence of this system is positive, since the polarizability along the main chain axis is larger than that measured perpendicular to it (the angle γ is *c.* 0°, which means $\alpha \sim \theta$). However, determination of the second-order Legendre polynomial from birefringence is usually difficult, since it requires a knowledge of the birefringence of a perfectly oriented polybutadiene (Δn_0) as a reference state, which is a rather uncertain quantity:

$$<P_2(\cos\alpha)> = \frac{\Delta n}{\Delta n_0} \qquad (11)$$

Although P_2 tends towards 1 for decreasing angles and towards −0.5 for 90°, it behaves linearly with angle for small orientations (small P_2 values around the magic angle). Since the experimental P_2 values as obtained from ^{2}H n.m.r. spectroscopy are very small, we can expect a similar birefringence behaviour and (negative)

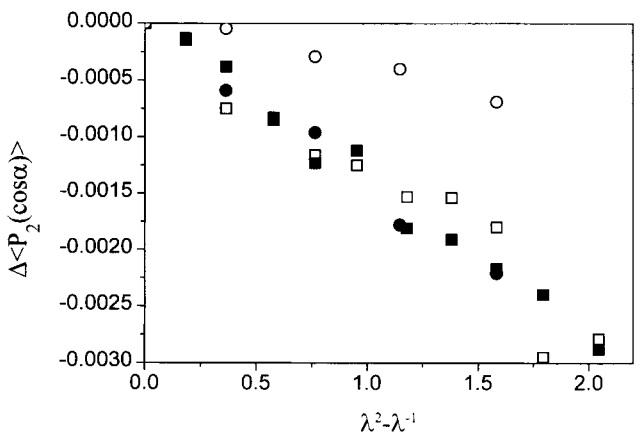

Figure 3 Corrected second-order Legendre polynomials for two different degrees of swelling, where open symbols represent oligomer, and closed symbols represent the network: squares, $\phi = 0.8$; circles, $\phi = 0.6$

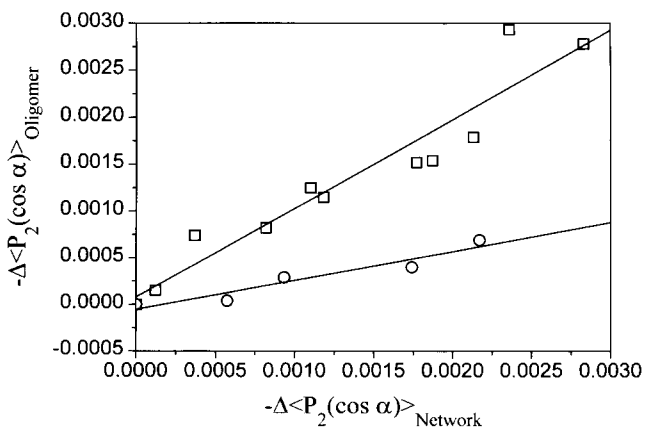

Figure 4 $-\Delta < P_2(\cos\alpha) >$ of oligomer as a function of $-\Delta < P_2(\cos\alpha) >$ of network: (□) $\phi = 0.8$; (○) $\phi = 0.6$

$\Delta < P_2(\cos\alpha) >$ values (from ^{2}H n.m.r. spectroscopy) as a function of strain. Thus we can use birefringence to check the validity of the correction procedure for the second-order Legendre polynomial obtained by n.m.r. spectroscopy. In *Figure 5* the negative second-order Legendre polynomials are shown for samples with $\phi = 0.8$ and 0.6, together with the birefringence. Since birefringence in this case is intrinsic (in contrast to birefringence induced by morphological anisotropies), it detects orientational phenomena on a short (segmental) length scale. From the similarity of the strain dependence in the case of the sample with $\phi = 0.8$, it can be concluded that the correction procedure for the Legendre polynomials outlined above is reasonable. (It should be noted that the identity of the values for Δn and $-\Delta < P_2(\cos\alpha) >$ is actually achieved by accident.) In the case of the sample with $\phi = 0.6$ the birefringence is located between the orientation values of the oligomer and the network. This is expected from comparison with the case where $\phi = 0.8$, since both the network and oligomer contribute to the birefringence. This is supported also by the fact that summation over the different contributions to $-\Delta < P_2(\cos\alpha) >$ obtained from ^{2}H n.m.r. spectroscopy yields the birefringence values (shown by open diamonds in *Figure 5b*) as follows:

$$\Delta< P_2(\cos\alpha)_{\lambda,\text{Sample}}> = \phi\,\Delta< P_2(\cos\alpha)_{\lambda,\text{Network}} > + (1-\phi)\,\Delta< P_2(\cos\alpha)_{\lambda,\text{Oligomer}} > \qquad (12)$$

In *Figure 6* we compare the dependence of the orientational coupling parameter, determined from the inner splitting by using equations (1) and (5) (open symbols) and from the whole spectra by using equations

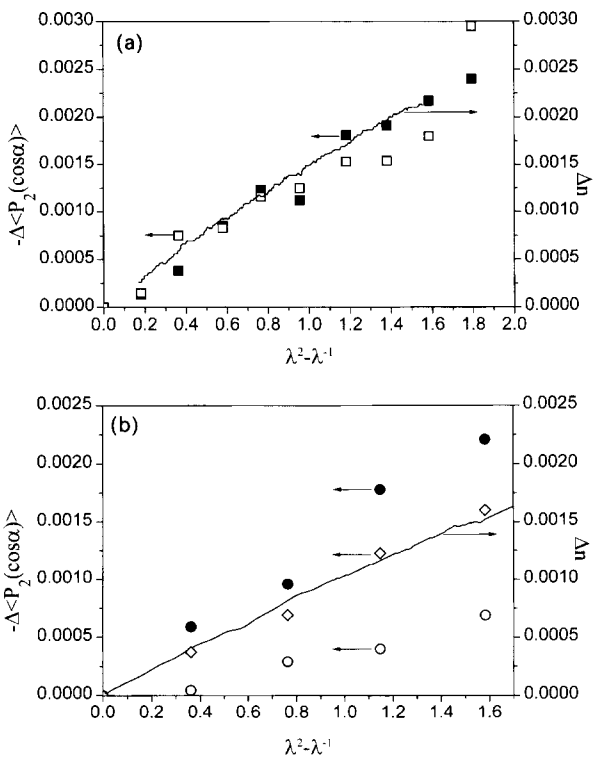

Figure 5 Negative corrected second-order Legendre polynomials together with the birefringence *versus* the strain function for network (■, ●) and oligomer (□, ○): (a) $\phi = 0.8$; (b) $\phi = 0.6$, where ◇ denotes the contribution of both network and oligomer according to equation (12)

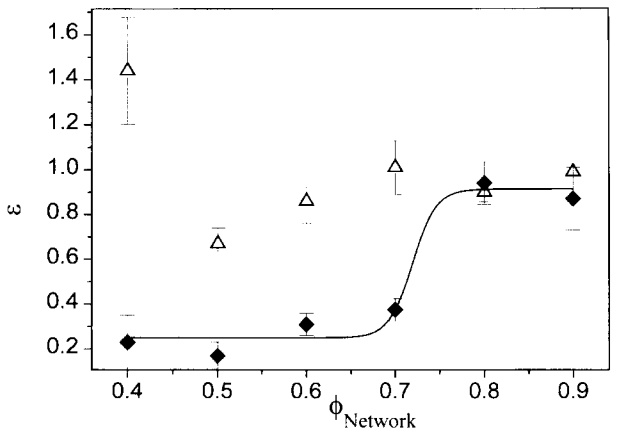

Figure 6 Dependence of the orientational coupling parameter on the degree of swelling: (△) from equations (1) and (5); (◆) from equations (1), (6), and (8)

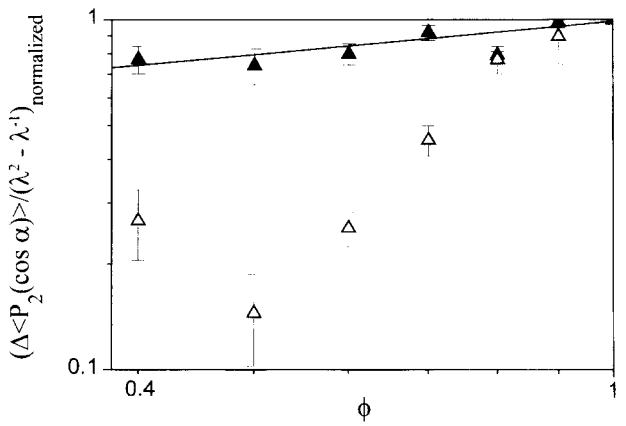

Figure 7 Normalized reduced orientation parameter as a function of the network volume fraction: (▲) network; (△) oligomer (the solid line has a slope of 1/3)

(1), (6), and (8) (closed symbols), on the degree of swelling. While the analysis of the quadrupolar splitting of the maxima yields some uncertainty in the concentration dependence of ϵ, the analysis of the whole spectra indicates an almost complete orientional coupling for low degrees of swelling ($\phi \geqslant 0.8$). An explanation for this result could be the presence of thermal motions in the sample which allow the oligomers to orient more randomly than the network chains. This should be the case when oligomer and network chains are not located right next to each other, as is expected at higher degrees of swelling. This result is in agreement with ref. 8, where a decrease of the orientational coupling parameter with descending values of ϕ was also found at $\phi \sim 0.7$. This concentration dependence of the orientational coupling is also shown in *Figure 7*, where the reduced orientation (as obtained from equations (1), (6), and (8), and then normalized with respect to the pure network ($\phi = 1$)) is plotted as a function of the volume fraction of the network. The reduced orientation of the network scales approximately with the cube root of the volume fraction of the network, which reflects the decrease of the crosslink density by adding the oligomer. This behaviour was also found for the mechanical stress[24]. As found in ref. 8, both oligomer and network show the same behaviour for small degrees of swelling. However, for larger degrees of swelling significant deviations occur between the orientations of the network and the oligomer (in ref. 8 only small degrees of swelling were studied).

CONCLUSIONS

These present experiments show that free chains below the entanglement molecular weight, which are structurally identical to the network matrix, show the same magnitude of segmental orientation upon uniaxial deformation as the network ($\epsilon = 1$) for small degrees of swelling. This supports the previous results obtained on polydimethylsiloxane[8] and polybutadiene[12] networks. For larger degrees of swelling, however, ϵ decreases, thus indicating a loss of correlation which can be attributed to increasing concentration fluctuations (local heterogeneities). Such heterogeneities have also been found in semi-interpenetrating polystyrene networks[35,36]. While in the previous ^{2}H n.m.r. spectroscopic studies only the quadrupolar splitting of the maxima in the spectra was used for determination of the second-order Legendre polynomial (P_2), we have used here the whole spectra to obtain the ensemble average of P_2. A comparison of the two ways to determine P_2 yields different results concerning the orientational coupling between oligomer and network for this system.

ACKNOWLEDGEMENTS

The authors are indebted to G. Person, S. Auerbach, J. Rösch, D. Oelfin and A. Hasenhindl for their help during the ^{2}H n.m.r. spectroscopic and birefringence measurements. Two of the authors (V.A. and R.S.) acknowledge a helpful discussion with H.-W. Spiess. This work has been supported by Stiftung Volkswagen-Werk through the joint project Freilburg (Germany)–Porto Algere (Brazil) and Deutsche Kautschuk-Gesellschaft (project 7/93). M.M.J. received a fellowship from Deutscher Akademischer Austauschdienst (DAAD), which is gratefully acknowledged. The authors also thank J. Hutchison for helpful comments on the manuscript.

REFERENCES

1 Deloche, B. and Samulski, E. T. *Macromolecules* 1981, **14**, 575
2 Deloche, B., Beltzung, M. and Herz, J. *J. Phys. (Paris) Lett.* 1982, **43**, 763
3 Toriumi, H., Deloche, B. and Samulski, E. T. *Macromolecules* 1985, **18**, 304
4 Dubault, A., Deloche, B. and Herz, J. *Macromolecules* 1987, **20**, 2096
5 Dubault, A., Deloche, B. and Herz, K. *Prog. Colloid Polym. Sci.* 1987, **75**, 45
6 Samulski, E. T. *Polymer* 1985, **26**, 177
7 Sotta, P., Deloche, B., Herz, J., Lapp, A., Durand, D. and Rabadeux, J.-C. *Macromolecules* 1987, **20**, 2769
8 Sotta, P., Deloche, B. and Herz, J. *Polymer* 1988, **29**, 1171
9 Kornfield, J. A., Fuller, G. G. and Pearson, D. S. *Macromolecules* 1989, **22**, 1334
10 Doi, M., Pearson, D. S., Kornfield, J. A. and Fuller, G. G. *Macromolecules* 1989, **22**, 1488
11 Ylitalo, C. M., Fuller, G. G., Abetz, V., Stadler, R. and Pearson, D. S. *Rheol. Acta* 1990, **29**, 729
12 Ylitalo, C. M., Zawada, J. A., Fuller, G. G., Abetz, V. and Stadler, R. *Polymer* 1992, **33**, 2949

13 Gronski, W., Stadler, R. and Jacobi, M. M. *Macromolecules* 1984, **17**, 741
14 Poon, C. and Samulski, E. T. *Makromol. Chem. Macromol. Symp.* 1990, **40**, 109
15 Poon, C. and Samulski, E. T. *J. Non-Cryst. Solids* 1991, **131–133**, 509
16 Deloche, B. and Sotta, P. *Macromolecules* 1990, **23**, 1999
17 Brereton, M. G. *Macromolecules* 1993, **26**, 1152
18 Jacobi, M. M., Stadler, R. and Gronski, W. *Macromolecules* 1986, **19**, 2884
19 Stadler, R., unpublished results
20 Forster, F. *PhD Thesis* Albert-Ludwigs-Universität, Freiburg, 1990
21 Kornfield, J. A., Chung, G.-C. and Smith, S. D. *Macromolecules* 1992, **25**, 4442
22 Spiess, H. W. *Colloid Polym. Sci.* 1984, **261**, 193
23 Bühler, F., Stadler, R. and Gronski, W. *Makromol. Chem.* 1986, **187**, 1295
24 Jacobi, M. M., Abetz, V., Stadler, R., de Lucca Freitas, L. and Gronski, W. *Colloid Polym. Sci.* 1995, **273**, 544
25 Jacobi, M. M., Stibal, E. and Stadler, R. *Makromol. Chem. Rapid Commun.* 1986, **7**, 443
26 Jacobi, M. M. *PhD Thesis* Albert-Ludwigs-Universität, Freiburg, 1989
27 Jacobi, M. M. and Stadler, R. *Makromol. Chem. Rapid Commun.* 1988, **9**, 709
28 Erman, B. and Flory, P. J. *Macromolecules* 1982, **15**, 800
29 Erman, B. and Flory, P. J. *Macromolecules* 1982, **15**, 806
30 Erman, B. and Flory, P. J. *Macromolecules* 1983, **16**, 1608
31 Abe, Y., Tonelli, A. E. and Flory, P. J. *Macromolecules* 1972, **3**, 550
32 Hentschel, D., Sillescu, H., Spiess, H. W., Voelkel, R. and Willenberg, B. in 'Proceedings of the 19th Ampere Congress on Magnetic Resonance and Related Phenomena', (Eds K. H. Hausser, D. Schweitzer and H. Brunner), Heidelberg, 1976, p. 381
33 Abramowitz, M. and Stegun, I. A. 'Handbook of Mathematical Functions', Dover, New York, 1964
34 Dardin, A. *PhD Thesis* Johannes Gutenberg-Universität, Mainz, 1995
35 Antonietti, M. and Sillescu, H. *Macromolecules* 1985, **18**, 1162
36 Rösch, J., de Lucca Freitas, L. L. and Stadler, R. *Polym. Bull.* 1991, **25**, 397